Semiconductor electrodes. 13. Characterization and behavior of n-type zinc oxide, cadmium sulfide, and gallium phosphide electrodes in acetonitrile solutions

P. A. Kohl, and A. J. Bard

J. Am. Chem. Soc., **1977**, 99 (23), 7531-7539• DOI: 10.1021/ja00465a023 • Publication Date (Web): 01 May 2002

Semiconductor Electrodes. 13. Characterization and Behavior of n-Type ZnO, CdS, and GaP Electrodes in Acetonitrile Solutions

P. A. Kohl and A. J. Bard*

Contribution from the Department of Chemistry, University of Texas at Austin, Austin, Texas 78712. *Received May 16, 1977*

Abstract: The photoelectrochemical behavior of n-ZnO, n-CdS, and n-GaP single crystal semiconductor electrodes was investigated in acetonitrile which contained various electroactive compounds whose standard redox potential varied by over 3.2 V. The cyclic voltammograms of the n-type semiconductors in the dark and illuminated were compared to the Nernstian behavior at a Pt disk electrode. The photodissolution of the semiconductor electrodes did not occur until the electrode potential was well positive of the flat band potential. An underpotential was developed for the photooxidation of solution species at each semiconductor. A model for electron transfer at the semiconductor–solution interface is proposed which incorporates a surface state or intermediate level which can mediate electron transfer and surface recombination. The model is used to discuss previous work with semiconductors, electron transfer, and stabilization of the semiconductor surface.

Key factors in the utilization of semiconductor electrodes in electrochemical cells and devices, including those for solar energy conversion, are knowledge of the relative locations of the energy levels in the semiconductor and solution and an understanding of the role that surface states or intermediate levels in the band gap region may play in the charge transfer processes. This information has been obtained by studying the electrochemical properties of the semiconductor electrode in solutions containing different redox couples and assuming that the model of Gerischer[1] can be used to rationalize the observed current–potential (i–V) behavior. This model basically requires that charge transfer occur isoenergetically from the conduction or valence bands of the semiconductor to solution species. A number of such studies of different semiconductors in aqueous solutions[2-10] have shown that while this model is useful in locating the band positions, it is necessary to invoke intermediate levels or surface states within the band gap region to explain the i–V and spectroscopic behavior.

We have previously[11,12] discussed the advantages of using a nonaqueous solvent, such as acetonitrile (ACN), in studying the behavior of the semiconductors TiO_2 and Si. These include a much wider potential range (i.e., effective solvent band gap) for investigating the semiconductor behavior and the availability of a large number of well-characterized couples which undergo reversible one-electron transfer reactions at potentials throughout this range. Thus the studies on the n-TiO_2/ACN interface demonstrated the occurrence of reductions and oxidations of species whose standard potentials were located above the flat-band potential (V_{fb}) via the conduction band, and reduction of species, via an intermediate level or surface states, at potentials positive of V_{fb}. We should also mention the work of Landsberg et al.[13] which was primarily concerned with reductions at n-GaP in ACN at potentials negative of V_{fb}.

The work reported here deals with a study of the behavior of n-type ZnO, CdS, and GaP with ACN solutions. The location of the bands, the determination of V_{fb}, and the mapping of the band gap region is described and the behavior of these materials (which photodecompose in aqueous solutions) under irradiation is discussed. Finally a model which relates the interfacial charge transfer rate to competitive rates involving the conduction and valence bands and surface states is proposed.

Experimental Section

Low-resistivity single crystal semiconductors about 1 mm thick and polished with 0.5 μ alumina were used. The n-GaP and n-ZnO were obtained from Atomergic Chemicals (Long Island, N.Y.) and the n-CdS from National Lead. The (001), (001), and (111) faces were used for the n-ZnO, n-CdS, and n-GaP, respectively. Two ohmic contacts were made on each by electrodepositing indium from a 0.1 M $InCl_3$ solution on the back of the crystal. The n-GaP was heated in a hydrogen atmosphere for about 1 h following the In deposition at 400 °C to make the contact ohmic. In each case the current measured between the two contacts was directly proportional to the applied voltage and independent of polarity. A copper wire was connected to the ohmic contacts with conducting silver epoxy cement (Allied Products Corp., New Haven, Conn.). The back and sides of the crystal were then covered with insulating 5-min epoxy (Devcon Corp., Danvers, Mass.) and mounted on a small glass disk connected to a glass tube with silicone adhesive (Dow Corning, Midland, Mich.). The glass tube provided an insulated internal path for the wire from the electrode. There was no apparent chemical attack on the silicone adhesive from either the ACN or the etching solutions. The n-ZnO was first etched in H_3PO_4 and then in concentrated HCl, each for 15 s.[14] The n-CdS and n-GaP were etched in 11 M HCl for 1 min.

Most of the compounds used in this study were obtained from commercial sources. The $Ru(TPTZ)_2(ClO_4)_3$ (TPTZ = 2,4,6-tripyridyl-*s*-triazene) and $Ru(bpy)_3(ClO_4)_2$ were prepared as described previously.[15] Most of the compounds were recrystallized several times from an appropriate solvent and all have been previously characterized in this laboratory. Controlled potential coulometry was used with some compounds to transform them to the desired oxidation state. Polarographic grade tetra-*n*-butylammonium perchlorate (TBAP), which was dried for 3 days under vacuum, was used as the supporting electrolyte. The ACN was dried and purified as previously described.[16] A cyclic voltammogram was obtained at a platinum disk electrode at the beginning of each experiment to ensure the purity of the solutions and to locate the standard potential with respect to the reference electrode.

A three-compartment cell, similar to the previous design,[11] was used for the electrochemical measurements. The reference electrode was either a silver pseudoreference electrode, consisting of a silver wire in the supporting electrolyte solution and separated from the test solution by a medium porosity fritted-glass disk or a silver wire in a 0.1 M $AgNO_3$ solution separated from the main compartment by a porous Vycor glass junction. All values are reported vs. the aqueous SCE. The counter electrode for voltammetric measurements was a coiled platinum wire separated from the main compartment by a

Table I.[a] Peak Potentials for Reductions and Reoxidations of the Compounds Used in This Study at Pt and the Three n-Type Semiconductors in the Dark and Illuminated with White Light

	Pt		n-ZnO				n-CdS				n-GaP			
			Dark		Illuminated		Dark		Illuminated		Dark		Illuminated	
	E_{pa}	E_{pc}	E_{pa}	E_{pc}	E_{pa}	E_{pc}	E_{pa}	E_{pc}	E_{pa}	E_{pc}	E_{pa}	E_{pc}	E_{pa}	E_{pc}
Band gap				3.2 eV				2.45 eV				2.25 eV		
V_{fb}				−0.76 V				−0.85 V				−1.5 V		
$Ru(bpy)_3^{3+}$	1.33	1.27		0.16	0.63	0.45		−0.69	−0.25	−0.69		−0.12		−0.22
	−1.28	−1.34	−1.29	−1.42	−1.29	−1.42	−1.3	−1.39	−1.3	−1.39		−1.39		−1.4
	−1.47	−1.53	−1.48	−1.62	−1.48	−1.62	−1.49	−1.59	−1.49	−1.59		−1.57		−1.57
	−1.72	−1.78	−1.74	−1.87	−1.74	−1.87	−1.75	−1.84	−1.75	−1.84		−1.87		−1.87
$Th^{+\cdot}$	1.26	1.20		0.47		0.51		−0.72		−0.67				
$10\text{-}MP^{+\cdot}$	0.85	0.79		0.30	0.5	0.43		0.15		0.05		0.27	0.40	0.12
$TMPD^{+\cdot}$	0.25	0.19		−0.19		−0.19		−0.48		−0.12	2.9	−0.61	0.29	−0.57
$Ox\text{-}1^{+\cdot}$	−0.39	−0.45		−0.51	−0.41	−0.47		−0.63	−0.45	−0.54	1.95	−1.02	−0.69	−1.01
	−1.19	−1.31	−1.16	−1.37	−1.23	−1.37	−1.07	−1.43	−1.23	−1.45		−2.06	−1.81	−2.26
BQ	−0.49	−0.55		−0.83	−0.54	−0.83		−0.94	−0.62	−0.86	1.95	−1.74		−2.22
	−1.05	−1.78		−2.26	−1.84	−2.3		−2.06	−1.52	−1.93				
$Ru(TPTZ)_2^{3+}$	−0.77	−0.84	−0.75	−0.90	−0.75	−0.90	−0.46	−0.9	−0.75	−0.85	1.0	−1.44	−0.75	−1.40
	−0.94	−1.00	−0.90	−1.14	−0.90	−1.14	−0.46	−1.04	−0.90	−1.00	−1.71	−2.15	−2.00	−2.15
	−1.59	−1.67					−1.58	−1.70	−1.58	−1.70				
	−1.83	−1.90					−1.82	−1.90	−1.82	−1.90				
AQ	−0.91	−0.97	−0.88	−0.99	−0.90	−0.98	−0.83	−1.02	−0.93	−1.09	1.30	−1.70	−1.48	−2.08
	−1.50	−1.71	−1.49	−1.78	−1.61	−1.74	−1.48	−1.79	−1.61	−1.81		−2.16	−2.48	−2.78
A	−1.91	−1.97	−1.88	−1.95	−1.86	−1.97	−1.89	−1.95	−1.89	−1.95	−0.31	−2.31	−2.16	−2.3

[a] Abbreviations used in this table: Th, thianthrene; 10-MP, 10-methylphenothiozine; TMPD, *N,N,N',N'*-tetramethyl-*p*-phenylenediamine; Ox-1, oxazine-1; BQ, *p*-benzoquinone; AQ, anthraquinone; A, anthracene. All potentials are vs. SCE and at a scan rate of 0.2 V/s.

medium porosity fritted-glass disk. A large area platinum foil was used for capacitance measurements.

The cyclic voltammograms were obtained with a PAR 173 potentiostat and PAR 175 universal programmer (Princeton Applied Research Corp., Princeton, N.J.) and recorded on Houston Instruments (Austin, Texas) Model 2000 X-Y recorder. The capacitance measurements were made with an ac bridge which utilized a Wenking 61 RH potentiostat (G. Bank Electronik, F.R.G.) and Tektronix (Portland, Oreg.) Type 564 oscilloscope. The semiconductors were illuminated with a 450-W xenon lamp (Oriel Corp., Stamford, Conn.). Solutions were prepared under an inert helium atmosphere in a Vacuum Atmospheres Corp. (Hawthorne, Calif.) glove box. The cell was sealed air tight with silicone vacuum grease for work outside the glove box. Techniques of solution preparation and measurement generally followed those previously described. Positive feedback was employed to compensate for both the solution resistance and the internal resistance of the semiconductor. The concentrations of the electroactive species were always maintained below 2 mM to keep the faradaic currents small to minimize the uncompensated *iR* drop.

Results

The useful working range of ACN containing 0.1 M TBAP at a platinum electrode, i.e., the range of potentials over which no significant faradaic current flows, extends from at least +2.5 to −2.5 V vs. SCE. For n-ZnO and n-CdS in the dark the positive limit is greatly extended to potentials beyond +5 V. For the n-GaP, however, appreciable anodic current appeared at about +2.0 in the ACN/TBAP background solution. Capacitance measurements were made for potentials consistent with a depletion layer formed within the semiconductor electrode using either an ac bridge or from the charging current observed in this region during cyclic voltammetric potential sweeps. For the latter case the space charge region capacitance, C_{sc}, was obtained by dividing the charging current by the scan rate, v (V s^{-1}). These data were used in a plot of C_{sc}^{-2} vs. V according to the Schottky-Mott equation[17]

$$1/C_{sc}^2 = (V - V_{fb} - kT.e)2/(e\epsilon\epsilon_0 N_D) \quad (1)$$

where ϵ is the dielectric constant of the semiconductor, ϵ_0, the permittivity of free space, N_D, the donor density, e, the electronic charge, k, the Boltzmann constant, and T, the absolute temperature. The C_{sc} values obtained by both the bridge and cyclic voltammetry depended upon frequency. The slopes of the plots were similar, however, for both the ACN and aqueous solutions and yielded the following donor densities: 1×10^{18} (GaP), 2×10^{17} (ZnO), and 8×10^{15} cm^{-3} (CdS). In ACN the deviations of the intercept with changing frequency were greater than those found for aqueous solutions and generally the reproducibility of duplicate trials at a given frequency was poorer for ACN than for aqueous solutions. Such frequency effects on the Schottky-Mott plots have been noted earlier and discussed; see, for example, Gomes et al.[18] and references cited therein. Consistent values of V_{fb} could not be obtained from these measurements and V_{fb} was estimated from the photocurrent measurements as described later.

Cyclic voltammetry at the semiconductor electrode in the dark and under illumination was carried out for a number of compounds and the results compared to those obtained with a platinum electrode immersed in the same solution. The wave shapes and peak potentials (E_p) were dependent upon the scan rate (v) when the electrode reactions were irreversible or when an insulating film developed on the electrode surface; usually a scan rate of 0.2 V/s was employed. The E_p values at Pt, n-ZnO, n-CdS, and n-GaP are summarized in Table I and are illustrated, along with the proposed band energies, in Figure 1. The results for each semiconductor are described in more detail in the following sections.

n-ZnO. In aqueous solutions ZnO undergoes photodecomposition to Zn^{2+} and O_2 when irradiated with light with an energy greater than band gap (3.2 eV).[1] The *i*-V curve for ZnO in ACN-0.1 M TBAP under illumination is shown in Figure 2a. A very small photoanodic current is observed at potentials of about −0.75 V, which is just positive of the value taken as V_{fb}. The photocurrent increases sharply, however, at potentials above about +0.5 V. This large photocurrent is also found when redox couples are added to the solution. A scan to negative potentials after carrying out photooxidation of the electrode at potentials more positive than +0.5 V resulted in

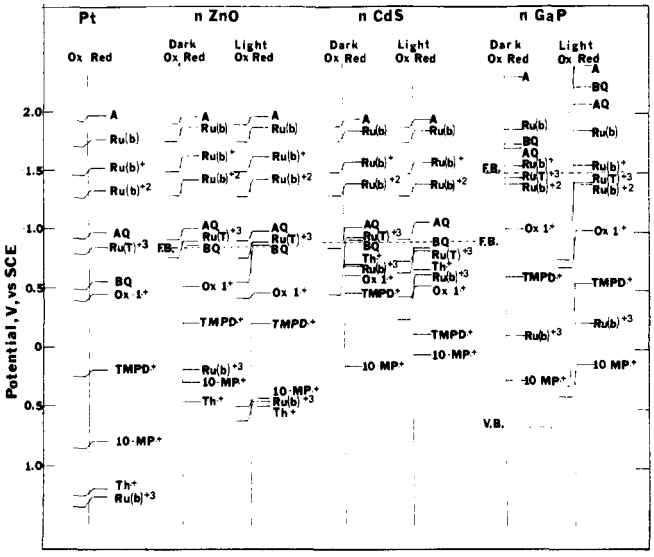

Figure 1. The reduction and reoxidation peak potentials for some of the compounds used in this study at a Pt disk electrode and at the three semiconductor electrodes in the dark and illuminated with white light. The scan rate was 0.2 V/s and the supporting electrolyte was 0.1 M TBAP.

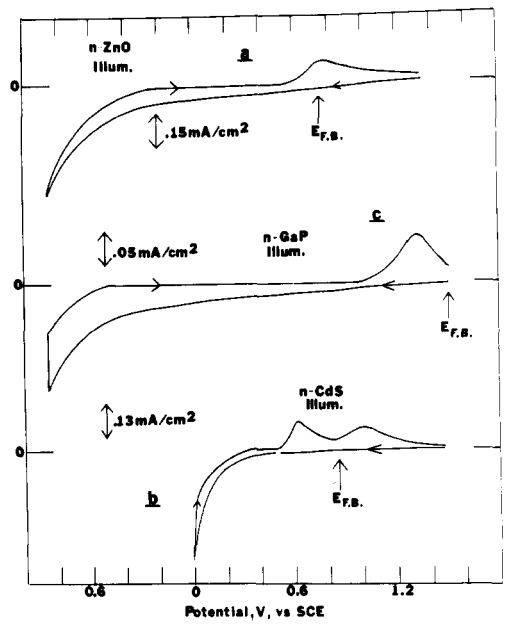

Figure 2. Cyclic voltammogram starting at negative potentials of the background photooxidation and rereduction of the semiconductor electrodes when illuminated with white light: (a) n-ZnO, (b) n-CdS, and (c) n-GaP. The scan rate was 0.2 V/s and the supporting electrolyte was 0.1 M TBAP.

the appearance of a reduction peak whose size and exact location depended upon the conditions of the photooxidation. This peak, which represents reduction of the photooxidation products of the ZnO, was not investigated further. If the electrode was held at a potential more positive than −0.2 V and illuminated with a light pulse of several seconds duration, an anodic current was observed which decayed with time. When the light was turned off, a small cathodic (dark) current was observed. For potentials between −0.2 and −0.75 V, a small photoanodic current was observed but no cathodic peaks were found during the light-off cycle.

The general cyclic voltammetric behavior of various substances at n-ZnO in ACN resembles that at n-TiO_2[11] and can be classified according to the potential region for the redox reaction at a platinum electrode. Substances which are reduced at potentials negative of V_{fb}, such as $Ru(bpy)_3^{2+}$ (Figure 3), do so under conditions where an accumulation layer has formed at the semiconductor surface. The onset of degeneracy of the surface produces metal like behavior of the semiconductor and similar cyclic voltammetric behavior is observed for Pt and ZnO. Thus the reversible three-step reduction of $Ru(bpy)_3^{2+}$ observed on Pt[15] is also seen at ZnO at essentially the same potentials but with a slightly larger separation of peak potentials between the cathodic and anodic waves. Similar results are obtained for the reduction of anthracene to the radical anion. Since irradiation of a moderately doped n-type electrode does not alter appreciably the density of electrons at the surface, especially at potentials well negative of V_{fb}, no effect of light on the i–V behavior is expected in this region. Small effects are indeed observed, however, which can be attributed to some heating at the electrode surface, resulting in convection of the solution and deviation of the current-time behavior from that expected for only diffusional mass transfer; similar effects can be found with platinum electrodes under irradiation. Decreases in the internal resistance of the semiconductor cause small sharp cathodic current spikes to appear when the light is turned on for potentials corresponding to the rising portion of the reduction wave.

A second region of interest involves couples whose redox potential lies at or somewhat positive of V_{fb}. Thus AQ, which shows Nernstian behavior at Pt, at a potential near V_{fb} of ZnO shows both cathodic and anodic waves at ZnO with a ΔE_p of 0.11 V, which decreases to 0.08 V upon illumination. BQ, however, which is reduced reversibly at Pt at potentials slightly

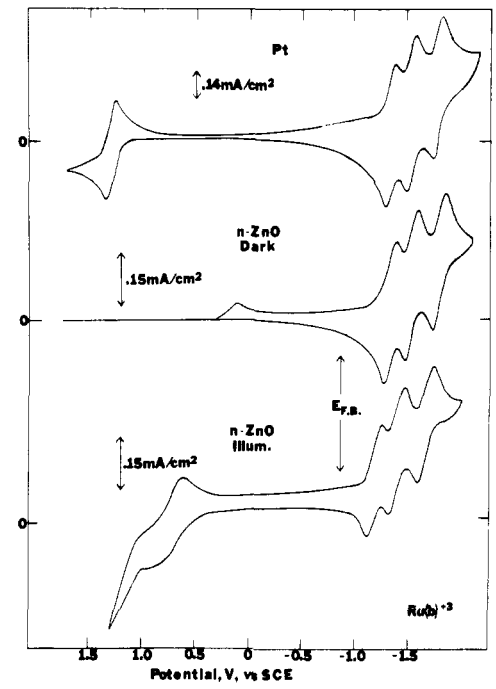

Figure 3. Cyclic voltammogram of a 1.0 mM solution of $Ru(bpy)_3^{3+}$ at a Pt disk electrode and single crystal ZnO electrode in the dark and illuminated with white light. The scan rate was 0.2 V/s.

positive of V_{fb}, shows an irreversible reduction at ZnO with the foot of the cathodic wave shifted almost to V_{fb} (Figure 4). Under illumination a reversal wave is observed, as well as the background ZnO oxidation at more positive potentials. It is interesting that a small reversal wave also appears for the second BQ reduction wave under illumination at ZnO, which appears to be more reversible than that seen at Pt. In general the behavior of BQ at ZnO resembles that found at TiO_2.[11] Similarly $Ox\text{-}1^{+}\cdot$, which shows two reversible reduction waves at Pt, shows an irreversible first reduction wave at ZnO shifted near, but positive of, V_{fb} (Figure 5). Again photooxidation of

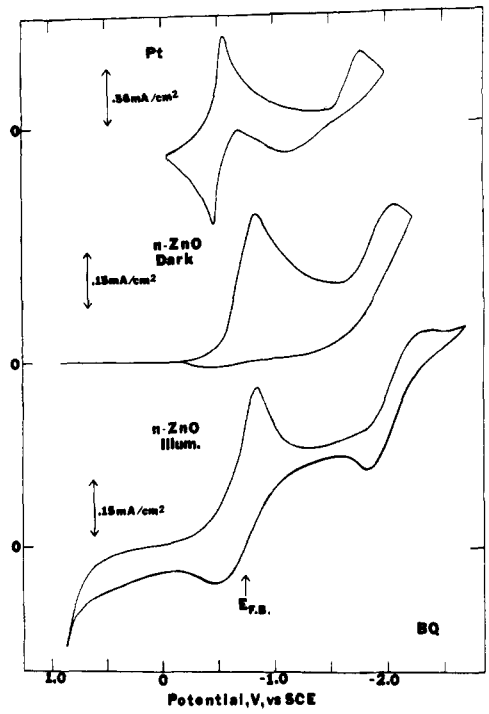

Figure 4. Cyclic voltammogram of BQ at a Pt disk electrode and single crystal ZnO electrode in the dark and illuminated with white light. The BQ concentration was 1.5 mM and the scan rate was 0.2 V/s.

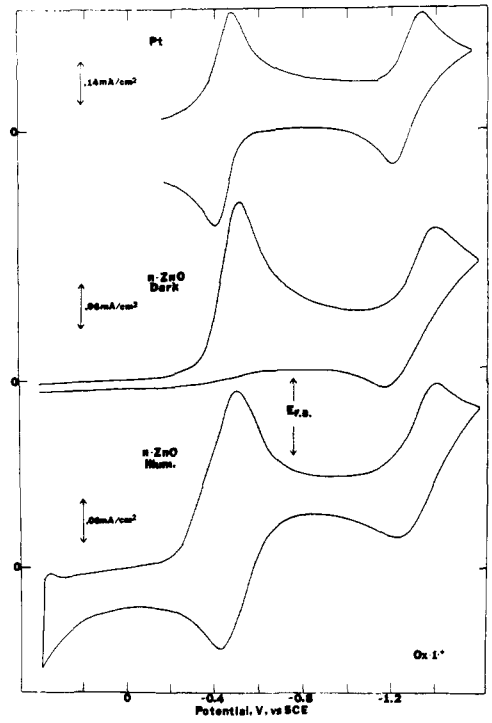

Figure 5. Cyclic voltammogram of a 1.0 mM solution of Ox-1^{+}· at a Pt disk electrode and single crystal ZnO electrode in the dark and illuminated with white light. The scan rate was 0.2 V/s.

the reduced form can occur under illumination. An experiment in which the electrode is irradiated by chopped light pulses during the potential sweep (i.e., linear scan voltammetry with periodic illumination) provides useful diagnostic information about the reaction pathway. In Figure 6 such an experiment is illustrated for Ox-1^{+}· with the potential scanned from negative to positive potentials at 10 mV/s. At potentials negative of V_{fb} the effect of the irradiation is the previously described thermal and electrode resistance effects on the reduction of

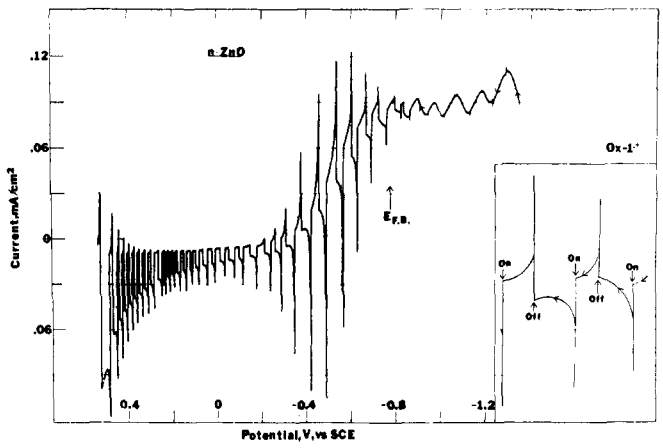

Figure 6. Potential sweep from negative to positive potentials of a 1.0 mM solution of Ox-1^{+}· at a ZnO electrode pulsed with white light as shown in inset. The sweep rate was 10 mV/s.

Ox-1^{+}·. Positive of V_{fb} each light pulse causes the oxidation of Ox-1, at potentials negative of where oxidation is observed on Pt, resulting in an anodic current spike decaying during the light-on pulse because of the decrease in the concentration of Ox-1 near the electrode surface and the increase of the cathodic back-reaction (Ox-1^{+}· reduction) as the Ox-1^{+}· concentration at the electrode surface increases. When the light pulse is turned off, a cathodic current spike is observed, representing the reduction of the photoelectrochemically generated Ox-1^{+}· near the surface. This general behavior is observed at potentials corresponding to the Ox-1^{+}· reduction wave. The size and shape of the current transients depend on the concentration profiles of Ox-1 and Ox-1^{+}· near the electrode surface, the rates of charge transfer, and the carrier distribution (i.e., the space charge region thickness) within the semiconductor.[19] The latter factor is important, because it controls the efficiency of capture of the incident radiation. At potentials just positive of V_{fb} the space charge region is narrow compared to the light penetration depth and smaller anodic photocurrents are observed compared to those at slightly more positive potentials, even though both potentials are negative of the cathodic E_p. A quantitative treatment of this behavior is under investigation. Note, however, that the peaks of the photocurrent transients trace out what approximates a cyclic voltammogram of the Ox-1^{+}·/Ox-1 system. At potentials at the foot of this wave (i.e., between 0 and −0.2 V) the anodic photocurrent decreases to that observed in the background solution, since Ox-1 is no longer produced during the dark periods. Finally, at more positive potentials starting at ca +0.3 V, the photooxidation of ZnO commences. Note that the onset of the anodic photocurrent spikes is useful in estimation of V_{fb}, which is thus located negative of −0.76 V. When a similar chopped-light experiment was performed with BQ and AQ, whose reductions occur negative of the flat band potential, only very small cathodic current overshoots were observed for BQ and none for AQ when the light was turned off at potentials just positive of V_{fb}.

The third region is composed of compounds reversibly reduced on platinum at potentials well positive of V_{fb}. These compounds ($Ru(bpy)_3^{3+}$, 10-MP^{+}·, Th^{+}·) are all irreversibly reduced at ZnO (Figure 1) with the reduction waves all occurring at potentials just negative of +0.5 V. This "leveling effect" is similar to that noted for n-TiO_2 for these compounds. For example, the $Ru(bpy)_3^{3+}$ reduction wave is shifted from when it occurs at Pt by well over 1 V (Figure 3). A chopped-light voltammogram of $Ru(bpy)_3^{3+}$ at ZnO is shown in Figure 7. The behavior generally follows that seen with Ox-1^{+}·, except that the wave occurs close to the current rise for ZnO photo-

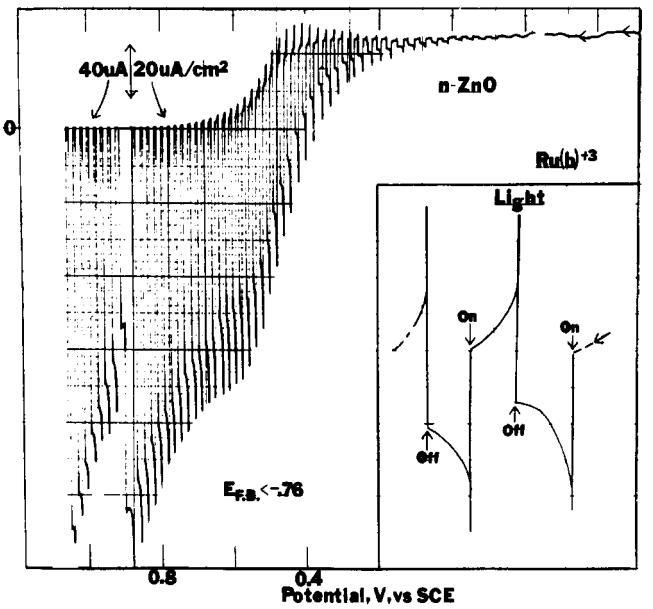

Figure 7. Potential sweep of a 1.0 mM solution of $Ru(bpy)_3^{3+}$ at a single crystal ZnO electrode pulsed with white light as shown in inset. The sweep was toward positive potentials at a rate of 10 mV/s.

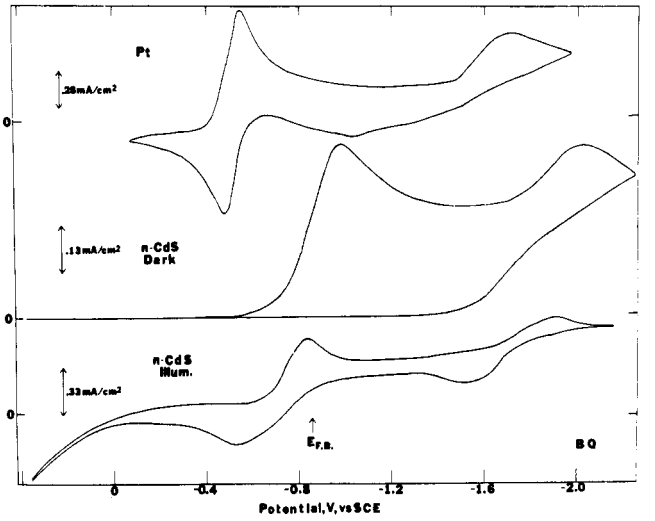

Figure 8. Cyclic voltammogram of a 1.5 mM solution of BQ at a Pt disk and single crystal CdS electrode in the dark and illuminated with white light. The scan rate was 0.2 V/s.

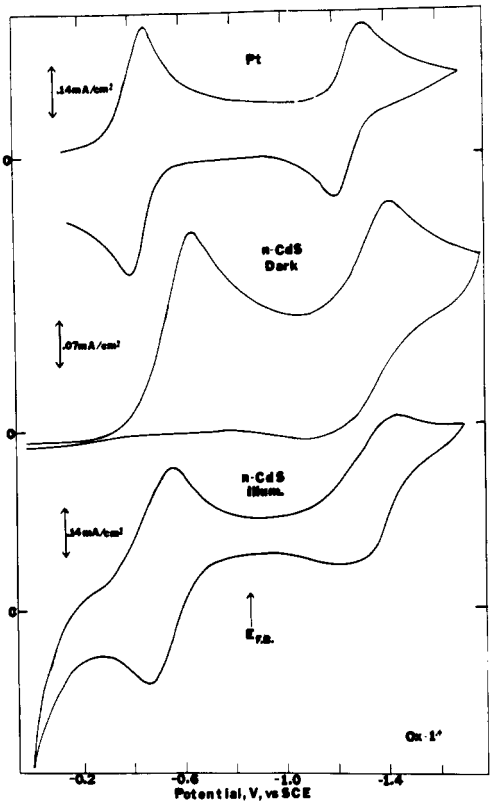

Figure 9. Cyclic voltammogram at 0.2 V/s of $Ox\text{-}1^{+}\cdot$ at a Pt disk electrode and single crystal CdS electrode in the dark and illuminated with white light. The $Ox\text{-}1^{+}\cdot$ concentration was 1.0 mM.

oxidation. Note that $Ru(bpy)_3^{2+}$ is photooxidized at ZnO at potentials negative of where oxidation occurs at Pt.

The reduction and subsequent photooxidation of $10\text{-}MP^{+}\cdot$ is similar to that of $Ru(bpy)_3^{3+}$, but it occurs at slightly more negative potentials. The photooxidation peak is more easily distinguished from the background oxidation because of this shift. Similar behavior was also observed for $Th^{+}\cdot$. However, for both $Th^{+}\cdot$ and $TMPD^{+}\cdot$ the ZnO surface could not be illuminated effectively because of the dark color of the solutions. When pulsed low-intensity light illuminated the electrode surface, small anodic currents were observed with no anodic or cathodic current overshoots.

n-CdS. The behavior of CdS was qualitatively similar to that of ZnO. In the background electrolyte a very small (<2 $\mu A/cm^2$) photooxidation is observed beginning at about −0.85 V. The sharp rise in the photocurrent, probably signaling the decomposition of the CdS lattice, begins at about −0.2 V (Figure 2b). A scan toward negative potentials following this photoanodization shows two cathodic peaks presumably due to reduction of lattice photooxidation products. When the electrode was illuminated with pulsed light of greater than band gap energy, both anodic and cathodic current overshoots appeared, even at potentials just positive of V_{fb}.

Compounds with redox potentials negative of V_{fb} showed reversible cyclic voltammograms on both Pt and n-CdS. Illumination of the electrode during reduction of these produced some convection in the solution, as discussed for ZnO. The presence of couples with redox potentials negative of V_{fb} had no effect on the anodic photocurrent observed positive of −0.85 V. The irreversible reduction of BQ (Figure 8) was again shifted to potentials negative of V_{fb} and the photooxidation of $BQ^{-}\cdot$ was superimposed on the small background photocurrent. Similarly, the irreversible reduction of $Ox\text{-}1^{+}\cdot$ (Figure 9) occurred at potentials positive of V_{fb} and the diffusion limited photooxidation of Ox-1 took place well positive of V_{fb}. A chopped-light voltammogram of $Ox\text{-}1^{+}\cdot$ at slow scan rates (10 mV/s) at CdS is very similar to that observed at ZnO (Figure 10). All compounds with redox potentials positive of V_{fb} are irreversibly reduced in the dark on n-CdS (Figure 1). A double wave appears during the reduction of Th^{+}. The first wave, which appears at −0.1 V, we attribute to the reduction of the products of the spontaneous oxidation of the semiconductor by the $Th^{+}\cdot$, while the second wave is the diffusion-limited irreversible reduction of unreacted $Th^{+}\cdot$ itself. The spontaneous oxidation is possible because the redox potential of the $Th^{+}\cdot/Th$ couple is probably positive of that for the reaction $Cd^{2+} + S + 2e = CdS$ (which is at +0.08 V vs. SCE in aqueous solution). The very large negative shift in the $Th^{+}\cdot$ reduction peak at CdS may be at least partly due to a change in the CdS surface during the spontaneous oxidation. Alternately the wave might be caused by a reaction product rather than $Th^{+}\cdot$ itself. However, a similar effect was observed for $Ru(bpy)_3^{3+}$ in which the second reduction peak in the dark occurred at −0.69 V and appeared to be the reduction of

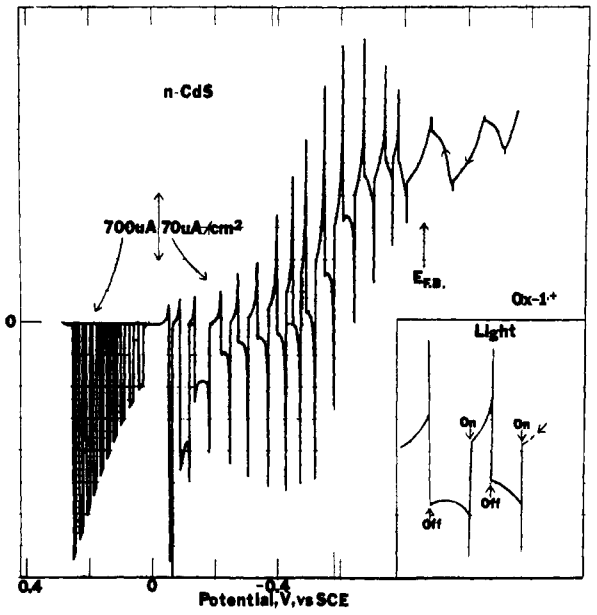

Figure 10. Potential sweep of a 1.0 mM solution of Ox-1^{+}· at a single crystal CdS electrode pulsed with white light as shown in inset. The sweep was toward positive potentials at 10 mV/s.

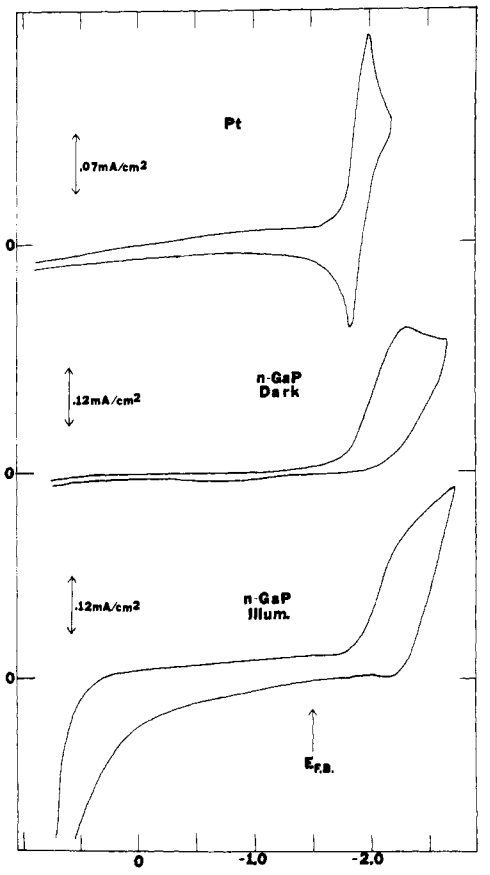

Figure 11. Cyclic voltammogram of a 0.35 mM solution of anthracene at a Pt disk electrode and n-GaP single crystal electrode in the dark and illuminated with white light. The scan rate was 0.2 V/s.

Ru(III). The Ru(II) was photooxidized just before the background photocurrent began.

n-GaP. Although the band gap of GaP, 2.25 eV, is near that of CdS, its V_{fb} is significantly more negative, and its behavior differs in several ways from that of ZnO and CdS. The *i*–V curve of GaP in background electrolyte solution under illumination is shown in Figure 2c. The onset of the large photoanodic current, again probably signaling lattice decomposition, does not occur until almost the valence band edge is reached. Unlike the results on ZnO or CdS, the reduction of compounds with potentials negative of V_{fb} occurs at waves that are irreversible both in the dark and under illumination. For example, anthracene is reduced in the dark at GaP at almost the same potential as is a Pt (Figure 11). However, no reoxidation is observed on scan reversal, and the behavior is only slightly different upon irradiation. Similar results were found by Landsberg and co-workers[13] for the reduction of aromatic hydrocarbons at n-GaP in ACN solutions. It appears that an insulating film forms on the GaP surface during the reduction[13] and that this film blocks any oxidation on reversal and also may hinder reductions on subsequent scans. This behavior complicates somewhat the interpretation of the results. For $Ru(bpy)_3^{2+}$, the three reduction steps were observed, but upon reversal the current decayed to zero at potentials near the second wave. AQ was also reduced in an irreversible wave, with only a small photooxidation peak apparent beginning at −1.6 V. Sharp anodic and cathodic current spikes were observed, however, when the GaP was irradiated with chopped light with the electrode held at potentials negative of V_{fb}. This may indicate that the film itself can be photooxidized thus allowing some current to flow before the film re-forms.

Compounds with standard potentials positive of V_{fb}, such as Ox-1^{+}· and $Ru(TPTZ)_2^{3+}$ (first reduction peak), showed irreversible cyclic voltammograms in the dark; these became quasi-reversible under illumination, with the photooxidation beginning at about −1.5 V. Chopped light again produced anodic and cathodic current spikes. In the dark, oxidation peaks occurring between +1.0 and +2.0 V were observed for several of the compounds with redox potentials in the band gap, as listed in Table I. This is attributed to band-to-band tunneling of electrons from the valence band to the conduction band. The irreversible reduction of 10-MP^{+}· on n-GaP occurs in a potential of about +1.7 V positive of V_{fb}, and about 0.5 V negative of its redox potential (Figure 12). Under illumination an oxidation wave for 10-MP appeared, and the cyclic voltammogram for the 10-MP^{+}·/10-MP system was constant and reproducible as long as the potential scan limits were between +0.6 and −1.2 V. Note that the photooxidation of 10-MP occurred with a "negative overpotential" (i.e., E_{pa} under irradiation at GaP − E_{pa} at Pt) of 0.45 V. When the potential of the GaP electrode was scanned to +1.0 V, where photodissolution of the electrode occurred, and the electrode surface changed causing cyclic voltammetric behavior of 10-MP and other couples to become less reversible (i.e., E_{pa} was shifted towards positive potentials and E_{pc} toward more negative ones).

Discussion

Location of V_{fb}. A knowledge of the position of V_{fb} is required to interpret the results. Although capacitance measurements as a function of potential for potentials positive of V_{fb} (for n-type semiconductors) and extrapolation using the Schottky–Mott equation have been employed, nonlinearity of the plots and variations of intercepts as functions of frequency introduce large uncertainties in the values of V_{fb} obtained. Problems of this kind have been noted in other studies[2,6,10,11,20-22] and have been ascribed to effects of surface states, adsorbed species, dielectric relaxation, residual faradaic currents, and surface roughness. The values of V_{fb} obtained by this method for n-type materials are frequently positive of the actual values.[2] These problems were also evident in the studies reported here.

The potential for the onset of the photoanodic current has often been taken as V_{fb}. However, the "onset" of any photooxidation depends to a large extent upon the current sensitivity

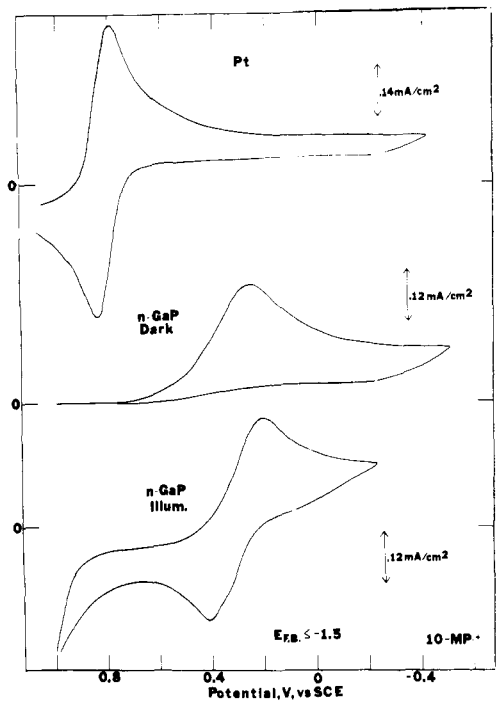

Figure 12. Cyclic voltammogram of 10-$MP^{+\cdot}$ at a Pt disk electrode and single crystal n-GaP electrode in the dark and illuminated with white light. The scan rate was 0.2 V/s and the 10-$MP^{+\cdot}$ concentration was 0.8 mM.

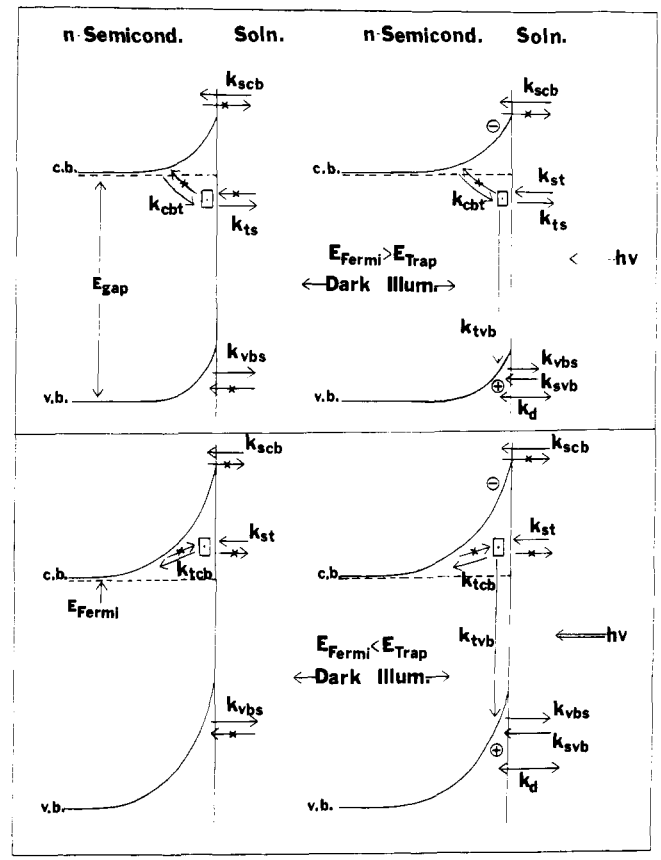

Figure 13. Proposed model for electron transfer at the n-type semiconductor/solution interface where the k's represent rate constants for electron transfer: k_{scb}, solution to the conduction band; k_{ts}, trap to solution; k_{st}, solution to trap; k_{cbt}, conduction band to trap; k_{tcb}, trap to conduction band; k_{tvb}, trap to valence band; k_{vbs}, valence band to solution; k_{svb}, solution to valence band. k_d is the rate constant for photodissolution of the semiconductor. E_{gap} is the band gap, c.b. represents the lower edge of the conduction band, and v.b. the upper edge of the valence band.

employed and the nature of the oxidation process. Thus, as we have shown here, the photoanodic dissolution of the semiconductor occurs only at potentials quite positive of V_{fb}, and extrapolation of the rising portion of the photoanodic current can lead to sizable errors. For example, past estimates of V_{fb} for ZnO in ACN based on this method led to values that were too positive.[13b,23,24] The results of the cyclic voltammetry studies and the potential for the photooxidations of $BQ^{-\cdot}$ and Ox-1 (see Figures 4-6) clearly place V_{fb} negative of −0.76 V vs. SCE. Thus V_{fb} can better be estimated by noting the potential where photooxidation first occurs for the compound which shows the most negative irreversible reduction; for ZnO and CdS, this compound was BQ.

Yet another method of determining V_{fb} is based on the open circuit photovoltage method.[17] Briefly, if the potential of an ideally polarized n-type semiconductor electrode is adjusted positive of the flat band potential, producing positive band bending, and then illuminated with light of energy greater than the band gap, the photogenerated holes and electrons are separated in such a way as to decrease the electric field in the space charge layer. The net effect is that the open circuit potential pulses in a negative direction toward the flat potential under illumination. Experiments of this type were performed for ZnO, CdS, and GaP in ACN using a battery to set the extent of band bending. A V_{fb} of −0.83 V was found by this technique for n-CdS. However, for n-ZnO the negative open circuit pulses were observed only for potentials positive of −0.3 V, while for n-GaP negative pulses were observed even at −2.6 V. Such "open-circuit" measurements can also be perturbed by the existence of and charge accumulation in surface states as well as the presence of the products of photodissolution which could lead to faradaic currents and photocorrosion of the electrode. The irreversible surface changes which occur at n-GaP as well as photoconductivity effects also complicate these types of measurements. Thus V_{fb} as located in these studies was based on the voltammetric measurements and the interpretation of the results is based on these values.

Proposed Model. The general behavior of ZnO and CdS follows that of TiO_2. The "leveling effect" in which compounds with redox potentials well positive of V_{fb} are reduced at about the same potentials within the band gap region can be explained by the existence of an intermediate level or surface states at this energy which mediate electron transfer between the semiconductor and the solution. These levels can also explain why the photodissolution occurs at potentials quite positve of V_{fb}. A representation of the overall model is shown in Figure 13, which also shows the rate constants for electron transfers between the intermediate level (t), the conduction band (cb), valence band (vb), and solution (s). Thus reductions of solution species at potentials positive of V_{fb} can occur at potentials near the surface level energy (E_t) and at a rate governed by k_{ts} and the rate at which the trap can be filled from electrons in the conduction band, which depends on k_{cbt}. This rate is a function of potential, and appears to be faster than the rate of diffusion of electroactive species to the electrode when the Fermi level is above E_t. Thus even for 60 mM 10-$MP^{+\cdot}$ a diffusion limited peak current was observed in voltammetric scans. The exact location of a reduction wave for a substance reduced via this level depends upon the nature of the overlap of the solution energy levels of the oxidized form with E_t.[1] When the Fermi level in the semiconductor becomes positive of the trap, the potential dependent rate becomes very slow and no further filling of the trap from the bulk of the semiconductor is possible. The dark oxidation of compounds irreversibly reduced is slow, however, probably because an energy barrier for electron transfer from the trap to the conduction band exists and is large, so that k_{tcb} remains small. From the voltammetric results

we place the location of the intermediate levels at about +0.5 V for ZnO and −0.2 V for CdS. The exact nature of these intermediate levels is not clear. In some cases they appear to be intrinsic to the material; for example, for n-TiO_2 the voltammetric results are very similar for single crystals and polycrystalline material prepared by several methods.[10,11] However, specific surface effects, such as specific adsorption, strong solvent interactions, or corrosion, might also govern the number and density of these levels. Moreover, one should probably think in terms of a series or continuum of levels rather than a single discrete one. Indeed the filling of the level from the conduction band might occur via a continum of surface states extending from E_t to the conduction band.[9]

When the electrode is illuminated and holes are photogenerated in the valence band, an additional rate constant, corresponding to the recombination of holes with electrons from the trap, k_{tvb}, is introduced. The photogenerated holes can also lead to the oxidation of the lattice at a rate k_d, which should be relatively potential independent. If the Fermi level is between the energy of the conduction band edge and E_t, in the absence of any electroactive species in solution, the photogenerated hole will either recombine with an electron from the trap or oxidize the lattice. The net rate of lattice decomposition thus depends upon the relative sizes of k_{tvb} and k_d. With the three semiconductors used here, electron transfer from the trap to the vb appears to compete very favorably with lattice decomposition and therefore the photoxidation of the lattice does not take place until the Fermi level is below E_t and the rate of filling of the trap from the cb becomes small. At this point recombination through the trap does not occur, and the lattice photooxidation is the dominant reaction. At n-ZnO, for example, the trap at +0.5 V mediates the recombination of photooxidzed holes and this inhibits dissolution as long as the potential is negative of this value. This explains the lack of rapid photodissolution of ZnO at potentials positive of V_{fb} but negative of +0.5 V. The trap level for n-CdS appears to be at about −0.2 V. The smaller anodic photocurrent observed for CdS compared to that found for ZnO when the electrode potential is between V_{fb} and E_t suggests that the ratio k_{tvb}/k_d is larger for n-CdS than for n-ZnO. The trap level on n-GaP appears to extend well into the band gap and almost to the valence band.

The addition of an electroactive species introduces other competitive rates. If the energy level of the reduced form overlaps the conduction band, then electron injection into it (dependent on k_{scb}) can occur even in the dark. If the overlap is with the surface state, then a species which could not be oxidized in the dark, because of the slow rate of emptying of the trap into the conduction band (i.e., a small k_{tcb}), can be photooxidized with the trap being filled by an electron from a solution species (rate constant, k_{st}). Even when the Fermi level is below E_t the rate of filling of the trap by a solution species and k_{tvb} can be large compared to k_d and the lattice decomposition can be decreased or eliminated. There has been much recent interest in the stabilization of semiconductors which photodecompose (e.g., CdS, CdSe, GaAs) by the addition of species to the solution which are preferentially oxidized (e.g., S^{-2}, Te^{2-}).[25-27] The rate of population of trap levels by the solution species, and thus the overlap of the energy levels of the reduced form of the redox couple with this level,[1] may then be determining factors in semiconductor stabilization. Indeed the relative rate of reaction of solution species with photogenerated holes compared to solvent and lattice oxidation for several redox couples has been studied for TiO_2[28] and CdS.[29] Both studies showed that redox couples with more negative redox potentials were more effective in competing for the photogenerated holes. These couples lie well away from the valence band edge, so that direct transfer to a hole in the valence band is unlikely. Better relative overlap with a surface state and photooxidation through it can, however, explain the results.[28] Stabilization may also depend upon specific interaction of the solution species with the electrode surface as well as the relative location of the solution redox level to the potential for decomposition of the semiconductor.[30] A quantitative model of these processes is currently under investigation.

We also noted positive shifts in the peak potentials for the reduction of 10-MP^+ and $Ru(bpy)_3^{3+}$ at ZnO when the electrode was illuminated. While part of this shift might be attributed to increases in the concentrations of the oxidized form at the electrode surface because of the photooxidation, increases in the rate of reduction via the intermediate level are also possible. The rate of reduction via the trap depends upon k_{cbt} and the surface concentration of electrons, n_s. At the potentials of the reduction process a strong depletion layer has formed and n_s is small. Under these conditions irradiation could cause an increase of n_s and hence facilitate reduction via the trap (n_s cannot be appreciably increased for potentials at or negative of V_{fb}). Since reduction reactions can also occur via these surface levels, the number and location of these may be important in the back-reaction of photogenerated oxidants which can decrease the overall quantum efficiency of the photoprocess at a semiconductor electrode. Note also that the photooxidation of some species, e.g., 10-MP or $Ru(bpy)_3^{2+}$ at ZnO, occurs at potentials very positive of V_{fb}. The usual model of the semiconductor electrode shows the photocurrent rising at potentials just positive of V_{fb}, with V_{fb} usually representing the most negative open circuit potential obtainable at the illuminated semiconductor. However, the occurrence of surface states within the band gap region which mediate electron transfer, especially if the photoactive redox couple is stable and reversible, holds the semiconductor potential at values near the surface state with the rise in photoanodic current not occurring until the electrode attains potentials where the back-reduction does not occur. In effect then these states can "pin" the potential of the semiconductor at or near E_t rather than at V_{fb}; this is somewhat analogous to the effect surface states have at a metal-semiconductor Schottky barrier.

Finally, we might discuss some luminescence experiments which are related to the results obtained here. For example, the recent study of the spectral distribution of electroluminescent emission from n-ZnO and n-CdS[9] by hole injection led to the conclusion that surface states played an important role in the radiative process. Similarly such states were proposed to explain luminenscence in n-GaP electrodes.[9,10] Two recent studies of the reduction of rubrene radical cation ($R^{+\cdot}$) at n-ZnO electrodes have appeared.[23,24] In one[23] direct reduction of $R^{+\cdot}$ to the triplet state was reported with subsequent emission of light while in the other[24] no emission was observed. Based on the results of the study here a possible reason can be proposed. The reduction of $R^{+\cdot}$ to the triplet state occurs at about −0.2 V vs. SCE (in benzonitrile). If the conduction band edge of ZnO in benzonitrile occurs at about the same potential as in ACN, i.e., ca. −0.8 V, then reduction occurs either via the surface state or through overlap with the conduction band. One difference in the conditions in the two experiments was the doping level of the ZnO: 2×10^{17} [23] vs. 3×10^{15} cm^{-3}.[24] If the rate of reduction depends upon k_{cbt} or on tunneling from the conduction band (which would be a function of space charge layer thickness and hence of doping level), rapid reduction via a level located in the band gap could be possible with one electrode but not with the other.

We close with some remarks concerning the use of nonaqueous solvents in devices utilizing semiconductor electrodes. A nonaqueous solvent will decrease the extent of photodecomposition of the semiconductor (i.e., shift E_D[30] to more positive potentials), if the solvation energy of the lattice ions

(e.g., Zn^{2+}, Cd^{2+}) is smaller in the solvent than in water. Moreover, many reversible couples are available in these solvents as additives for stabilizing the semiconductor. For example, in this study photooxidation of compounds such as 10-MP at potentials negative of the reversible redox potential at n-GaP was observed. These photoanodic currents were stable and reproducible, showing that the n-GaP was stabilized; only two other studies of photoprocesses at n-GaP in aqueous solution showed stable behavior.[31,32] Furthermore, the larger oxidation limits of the solvent allow more positive redox couples to be employed in photoelectrochemical cells, which allow greater output voltages and potentially higher efficiencies. However, as described above, surface states can also play the role of recombination centers for the redox processes of solution species. When these are important, the maximum potential available for a cell involving a solution containing a couple with a potential E_{redox}, an electrode reversible to the couple, and an n-type semiconductor will be decreased from $E_{redox} - V_{fb}$ to $E_{redox} - E_t$. When recombination via surface states is important, chemical etching of the semiconductor, which can lead to a change in the density of such states, may be useful in obtaining better efficiencies.

Acknowledgment. We wish to thank Dr. Steven N. Frank for his continuous interest in this work. The support of this research by the National Science Foundation and the Robert A. Welch Foundation is gratefully acknowledged.

Reference and Notes

(1) (a) H. Gerischer in "Physical Chemistry: An Advanced Treatise", Vol. 9A, H. Eyring, D. Henerson, and W. Jost, Ed., Academic Press, New. York, N.Y., 1970; (b) H. Gerischer, *Adv. Electrochem. Electrochem. Eng.*, **1**, 139 (1961).
(2) R. A. L. Vanden Berghe, F. Cardon, and W. P. Gomes, *Surf. Sci.*, **39**, 368 (1973).
(3) H. Kiess, *J. Phys. Chem. Solids*, **31**, 2379 (1970).
(4) H. Gerischer, *Surf. Sci.*, **18**, 97 (1969).
(5) H. Kokado, T. Nakayama, and E. Inoue, *J. Phys. Chem. Solids*, **35**, 1169 (1974).
(6) (a) R. A. L. Vanden Berghe, F. Cardon, and W. P. Gomes, *Ber. Bunsenges. Phys. Chem.*, **77**, 290 (1973); (b) *ibid.*, **78**, 331 (1974).
(7) V. A. Tyagai and G. Y. Kolbasov, *Surf. Sci.*, **28**, 423 (1971).
(8) K. H. Beckmann and R. Memming, *J. Electrochem. Soc.*, **116**, 368 (1969).
(9) B. Pettinger, H-R Schoppel, and H. Gerischer, *Ber. Bunsenges. Phys. Chem.*, **80**, 849 (1976).
(10) R. N. Noufi, P. A. Kohl, S. N. Frank, and A. J. Bard, *J. Electrochem. Soc.*, in press.
(11) S. N. Frank and A. J. Bard, *J. Am. Chem. Soc.*, **97**, 7427 (1975).
(12) D. Laser and A. J. Bard, *J. Phys. Chem.*, **80**, 459 (1976).
(13) (a) R. Landsberg, P. Janietz, and R. Dehmlow, *Z. Phys. Chem. (Leipzig)*, **257**, 657 (1976); (b) *J. Electroanal. Chem.*, **65**, 115 (1975); (c) *Z. Chem.*, **15**, 38, 106 (1975); (d) *ibid.*, **14**, 363 (1974).
(14) W. P. Gomes, T. Freund, and S. R. Morrison, *J. Electrochem. Soc.*, **115**, 818 (1968).
(15) N. E. Tokel-Takvoryan, R. E. Hemingway, and A. J. Bard, *J. Am. Chem. Soc.*, **95**, 6582 (1973).
(16) S. N. Frank, A. J. Bard, and A. Ledwith, *J. Electrochem. Soc.*, **122**, 898 (1975).
(17) V. A. Myamlin and Y. V. Pleskov, "Electrochemistry of Semiconductors", Plenum Press, New York, N.Y., 1967.
(18) (a) E. C. Dutoit, R. L. Van Meirhaeghe, F. Cardon, and W. P. Gomes, *Ber. Bunsenges, Phys. Chem.*, **79**, 1206 (1976); (b) W. H. Laflere, R. L. Van Meirhaeghe, T. Cardon, and W. P. Gomes, *Surf. Sci.*, **59**, 401 (1976).
(19) D. Laser and A. J. Bard, *J. Electrochem. Soc.*, **123**, 1837 (1976).
(20) (a) W. P. Gomes and F. Cardon, *Ber. Bunsenges. Phys. Chem.*, **74**, 432 (1970); (b) E. C. Dutoit, R. L. Van Meirhaege, F. Cardon, and W. P. Gomes, *ibid.*, **79**, 1206 (1976).
(21) B. Pettinger, H. R. Schoppel, T. Yokoyama, and H. Gerischer, *Ber. Bunsenges. Phys. Chem.*, **78**, 1024 (1974).
(22) D. Elliot, D. L. Zellmer, and H. A. Laitinen, *J. Electrochem. Soc.*, **117**, 1343 (1970).
(23) L. S. R. Yeh and A. J. Bard, *Chem. Phys. Lett.*, **44**, 335 (1976).
(24) E. W. Grabner, *Electrochim. Acta*, **20**, 7 (1975).
(25) (a) A. B. Ellis, S. W. Kaiser, and M. S. Wrighton, *J. Am. Chem. Soc.*, **98**, 6418 (1976); (b) *ibid.*, **98**, 1635 (1976); (c) *ibid.*, **98**, 6855 (1976).
(26) B. Miller and A. Heller, *Nature (London)*, **262**, 680 (1976).
(27) G. Hodes, J. Manassen, and D. Cahen, *Nature (London)*, **261**, 403 (1976).
(28) S. N. Frank and A. J. Bard, *J. Am. Chem. Soc.*, **99**, 4667 (1977).
(29) T. Inoue, T. Watanabe, A. Fujushima, K. Honda, and K. Kohayakawa, *J. Electrochem. Soc.*, **124**, 719 (1977).
(30) A. J. Bard and M. S. Wrighton, *J. Electrochem. Soc.*, in press.
(31) Y. Nakato, K. Abe, and H. Tsubomura, *Ber. Bunsenges. Phys. Chem.*, **80**, 1002 (1976).
(32) A. B. Ellis, J. M. Bolts, S. W. Kaiser, and M. S. Wrighton, *J. Am. Chem. Soc.*, **99**, 2848 (1977).

Stereochemical Nonrigidity in Solid Zirconium and Hafnium Tetrakistetrahydroborates. Evidence for Two Dynamic Intramolecular Rearrangement Processes in Covalent Tridentate Tetrahydroborates

I-Ssuer Chuang, Tobin J. Marks,* [1] William J. Kennelly, and John R. Kolb

Contribution from the Department of Chemistry and the Materials Research Center, Northwestern University, Evanston, Illinois 60201. *Received March 21, 1977*

Abstract: Proton nuclear magnetic resonance studies of stereochemical dynamics in $Zr(BH_4)_4$ and $Hf(BH_4)_4$ have been carried out in the solid state. Variable temperature investigations were conducted in both continuous wave and pulsed modes. Two intramolecular motional processes were identified for each complex and the nature of these processes was interpreted on the basis of effective second moment calculations in both diffusive and positional jump regimes. The higher temperature process is assigned to rapid intramolecular bridge-terminal hydrogen exchange, $E_a(Zr) = 5.2 \pm 0.3$ ($\Delta G^{\ddagger} = 8.1$ at 214 K) l; $E_a(Hf) = 8.4 \pm 0.3$ ($\Delta G^{\ddagger} = 7.3$ at 200 K) kcal/mol. The lower temperature motion is suggested to involve rapid threefold rotation about the ligand M–B–H (terminal) axis with $E_a(Zr) = 5.4 \pm 0.2$ ($\Delta G^{\ddagger} = 4.3$ at 124 K) l; $E_a(Hf) = 4.6 \pm 0.2$ ($\Delta G^{\ddagger} = 4.4$ at 133 K) kcal/mol.

Although nuclear magnetic resonance spectroscopy has been employed to study motional processes in the solid state for a number of years,[2] two relatively recent developments promise to markedly increase activity in this area. The first is the elegant refinement of multiple pulse techniques for acquiring high-resolution information for magnetically dilute nuclei.[3] The second is the discovery that dynamic phenomena more elaborate than simple bond rotation (e.g., of methyl groups), molecular reorientation, or molecular diffusion can be observed and analyzed in the solid state. Among these more